Frontiers in Bioscience Landmark

Front. Biosci. (Landmark Ed) **2026**; 31(3): 48405
https://doi.org/10.31083/FBL48405

Short Communication

Synergistic Anticancer Activity of Dual-Molecule-Loaded Polymeric Films Based on Hyaluronic Acid Against Melanoma

Polina G. Serbun[1], Svetlana N. Morozkina[1,2,3], Roman O. Shaikenov[1], Ksenia S. Zavkibekova[4], Elena A. Vinogradova[4], Anna V. Motorzhina[4], Kateryna V. Levada[4], Hao Wu[1,5], Jingran Zhang[5,6], Zuobin Wang[5,7], Petr P. Snetkov[1,3,*]

[1]Institute of Advanced Data Transfer Systems, ITMO University, 197101 St Petersburg, Russia
[2]Progressive Materials and Additive Technologies Center, Kabardino-Balkarian State University Named After H.M. Berbekov, 360004 Nalchik, Russia
[3]Institute of Medicine, Saint Petersburg State University, 199034 St Petersburg, Russia
[4]REC Smart Materials and Biomedical Applications, Immanuel Kant Baltic Federal University (IKBFU), 236016 Kaliningrad, Russia
[5]International Research Centre for Nano Handling and Manufacturing of China, Changchun University of Science and Technology, 130022 Changchun, Jilin, China
[6]Ministry of Education Key Laboratory for Cross-Scale Micro and Nano Manufacturing, Changchun University of Science and Technology, 130022 Changchun, Jilin, China
[7]Centre for Opto/Bio-Nano Measurement and Manufacturing, Zhongshan Institute of Changchun University of Science and Technology, 528437 Guangzhou, Guangdong, China
*Correspondence: ppsnetkov@itmo.ru (Petr P. Snetkov)
Academic Editors: Kota V. Ramana and Roberto Bei
Submitted: 20 November 2025 Revised: 11 February 2026 Accepted: 3 March 2026 Published: 23 March 2026

Abstract

Background: Melanoma, an aggressive cancer with a poor prognosis, is difficult for early diagnosis, and there are limited drug treatments. Biologically active molecules, especially polyphenols and flavonoids, have a great therapeutic potential; however, their applications are limited by low aqueous solubility and bioavailability. **Research Design and Methods**: The mixture of usnic acid and curcumin was loaded into the polymer matrices based on hyaluronic acid, with the following polymeric film casting. The anticancer activity of the dual-molecule-loaded polymeric films was evaluated against lightly pigmented human melanoma SK-MEL 28 and unpigmented melanoma CVCL-7036 in comparison with the immortalized human keratinocytes HaCaT. **Results**: Usnic acid/curcumin-loaded biopolymer matrices demonstrated a high selective antitumor toxicity against melanoma SK-MEL 28 and CVCL-7036 cell lines with high biocompatibility with immortalized human keratinocytes HaCaT. **Conclusions**: Results highlight the potential of the obtained dual-molecule-loaded thin films based on hyaluronic acid as topical and safe antitumor therapy systems for local administration for the melanoma treatment. Moreover, due to the intrinsic properties of usnic acid and curcumin, and the biological activity of native hyaluronic acid, it is supposed that the obtained matrices possess the anti-inflammatory, antioxidant, antibacterial, and wound-healing activities, which are planned to be confirmed in further investigations.

Keywords: hyaluronic acid; curcumin; melanoma; drug synergism; usnic acid

1. Introduction

Melanoma is an aggressive type of skin cancer that rapidly metastasizes, and despite the possibility of being detected in only 5–10% of patients, it demonstrates a mortality equal to 90%. It primarily revealed patients with pale skin and with atypical moles or large numbers of benign moles [1], with an average diagnosis age of 57–69 years. However, a third of all diagnosed cases of melanoma are often found in young people [2]. Genetic factors and environmental conditions, especially ultraviolet radiation, are the dominant factors for carcinogenesis development [3].

Malignant melanoma typically arises from a benign melanocytic nevus through mitotic mutations in normal melanocytes caused by ultraviolet-induced DNA damage. UVB irradiation (280–320 nm) causes direct DNA damage with disruptions in tumor suppressor genes (such as *TP53*) and oncogenes (e.g., human gene that encodes a protein called B-Raf (*BRAF*)). UVA irradiation (320–400 nm) generates reactive oxygen species (ROS), leading to the oxidative damage of DNA, causing mutations in tumor suppressor genes (e.g., *PTEN*). These gene mutations dysregulate the signaling pathways, such as MAPK/ERK, PI3K/AKT, and P53, allowing cancer cells to overcome apoptosis, become immortal, and begin to metastasize [4–6]. Further tumor growth is supported by the microenvironment, where keratinocytes and fibroblasts affect the proliferation and viability of cancer cells through stem cell factor (SCF) and endothelin 1 (EDN1) factors [7]. Moreover, melanoma has strong immune evasion by PD-L1 and cytotoxic T-lymphocyte-associated protein 4 (CTLA-4) expres-

sions that suppress the activity of T-killers, accelerating the growth of the tumor and decreasing the drug sensitivity [8].

Melanoma has a high mutational burden, representing both germline and somatic mutations, leading to cancer cell heterogeneity and multidrug resistance, accelerating the tumor progression from primary lesions to invasion and metastasis [9]. Germline mutations in the *CDKN2A* gene, which encodes the tumor suppressor protein p16INK4a, cause hereditary susceptibility to melanoma through an autosomal dominant type and increase the risk of the negative impact of environmental factors such as ultraviolet radiation for carcinogenesis [1]. The microphthalmia-associated transcription factor (MITF) plays a key role in the regulation of melanocyte activity. The MITF factor influences melanocyte function by its involvement in phenotypic plasticity and the regulation of MAPK signaling and DNA repair [10]. *MITF* gene mutations, prevalently somatic, are often associated with alterations in the *PTEN* tumor suppressor gene, and its dysregulation leads to disruptions in the PI3K/AKT signaling pathway, resulting in uncontrolled cancer cell proliferation, increased cell immortality, and abnormal metabolic processes. These alterations are generally related to advanced-stage tumors with poor prognosis for patients [4,7].

The development of new therapeutic strategies for melanoma treatment is challenging due to the limited efficacy of traditional pharmaceutical cytostatic anticancer agents such as dacarbazine and temozolomide, which demonstrate low therapeutic effectiveness and minimal survival benefit in melanoma compared to other types of cancers. Immunotherapy and radiotherapy seem to be more promising [11], while natural biologically active agents, especially polyphenols and flavonoids, have attracted interest as a potential synergic component or even individual alternative for traditional anticancer agents. For example, pterostilbene induces melanoma cells apoptosis by pro-apoptotic gene upregulation and caspase activation [12], gracillin activates autophagy by inhibiting the PI3K/AKT/mTOR pathways and mitochondrial function [13], curcumin modulates multiple signaling pathways which reduce cancer cell proliferation, promote apoptosis, and decrease oxidative DNA stress [14,15], usnic acid demonstrate anti-proliferative, pro-apoptotic, anti-angiogenic, and photoprotective activities combined with downregulating PD-L1 and disrupt melanoma cell migration. Moreover, usnic acid is able to reduce melanoma cell viability and increase the cytotoxic effect of chemotherapeutic drugs, such as doxorubicin [16–18]. Thus, previous studies highlight the application potential of biologically active agents in melanoma treatment strategies through several mechanisms.

In this article, we describe the results of anti-cancer activity obtained for the dual-molecule-loaded polymeric films against lightly pigmented human melanoma SK-MEL 28 and unpigmented melanoma CVCL-7036 in comparison with the immortalized human keratinocytes HaCaT.

2. Materials and Methods

2.1 Materials

Hyaluronic acid 1.3 MDa (Rensin Chemicals Limited, Nanjing, Jiangsu, China) and 2.5 MDa (Amhwa Biopharm Co., Ltd., Binzhou, Shandong, China); curcumin, and usnic acid (abcr GmbH, Karlsruhe, Germany); dimethyl sulfoxide (DMSO, JSC EKOS-1, Moscow, Russia); distilled water (obtained using a laboratory distillation apparatus) were used.

2.2 Preparation of Polymeric Films

The polymeric films were prepared by the film casting method from 1.5 wt.% hyaluronic acid polymer solutions. Briefly, hyaluronic acid was dissolved in an equivoluminal mixture of distilled water and dimethyl sulfoxide. Curcumin and usnic acid were loaded into polymeric solutions with the weight ratio to hyaluronic acid equal to 1:15 and 1:30, respectively. The resulting polymer solutions were poured out into Petri dishes and stabilized at 24 °C overnight. At the final stage, the Petri dishes were placed in a drying chamber at 40 °C × 48 h.

2.3 Cell Cultures

The HaCaT cell line was obtained from the Russian Collection of Cell Cultures (Institute of Cytology RAS, St. Petersburg, Russia). Melanoma cell lines CVCL-7036 and SK-MEL 28 were kindly provided by the Laboratory of Biochemical Foundations of Pharmacology and Tumor Models (N. N. Blokhin Russian Cancer Research Center). All cell lines were validated by STR profiling and tested negative for mycoplasma. Cells were cultured in Dulbecco's modified Eagle's medium (DMEM) supplemented with 10% fetal bovine serum (FBS) and 1% penicillin/streptomycin (P/S) ((all Sigma-Aldrich, St. Louis, MO, USA). The cultivation was performed in an incubator (CO_2 incubator Galaxy 170 S, New Brunswick, UK) at 37 °C in an atmosphere with 5% CO_2. The fourth and fifth cell passages of cells were used for the experimental manipulations.

2.4 Compositions of the Studied Samples

For the experiments, the samples of films based on high-molecular hyaluronic acid with a molecular weight of 1.3 MDa and 2.5 MDa, with the addition of curcumin (CUR) in the ratio of 15 to 1 (by weight), respectively, as well as the samples of hyaluronic acid (HA) with CUR and usnic acid (USN) in a ratio of 15:1:0.5, respectively, were used. The compositions of the HA 1.3 group samples are presented in **Supplementary Table 1**.

The compositions of the samples of the group HA 2.5 are presented in **Supplementary Table 2**.

Samples were dissolved in distilled water at a concentration of 1.0 mg/mL. Then a series of dilutions was carried out to achieve the studied concentrations of 100, 50, and 10 µg/mL in DMEM medium. The molar concentrations of the active substances in the solutions of the samples of the HA 1.3 group are presented in **Supplementary Table 3**.

2.5 Cells Viability Test

The WST-1 test was used to assess cell viability. Cells were seeded in 96-well plates at 1×10^4 cells per well in 100 µL of DMEM medium and stored overnight. To exclude the influence of the studied material and the nutrient medium, wells with the cell medium and test solutions in the cell medium were additionally seeded. Each experiment was carried out in six repetitions. After 72 h of incubation with sample solutions, 10 µL of WST-1 reagent was added to each well, and the plate was incubated for two hours under the standard conditions. The optical density was measured at the wavelength of 450 nm using the plate spectrophotometer (Multiskan FC Microplate Photometer, Thermo Fisher Scientific, Waltham, MA, USA).

2.6 Cell Migration Study Using the Wound Healing Assay

The wound healing assay was used to evaluate keratinocyte migration [19]. HaCaT and SK-MEL 28 cells were seeded at 3×10^5 cells per well of a six-well plate in DMEM. After 48 h of monolayer formation, the cells were washed with PBS and scratched with a 1.0-milliliter tip. The medium in all wells was then replaced with depleted DMEM (1% FBS, 1% P/S), and sample solutions were added to the experimental wells. For HaCaT cells, samples from group HA 1.3 were used at a concentration of 50 µg/mL, and for SK-MEL 28 cells, solutions of HA 2.5 CUR USN and HA 2.5 USN were used at a concentration of 100 µg/mL. Three to six replicates were performed for each sample. Microphotographs of the same area were taken at $\times$20 magnification at 0, 3, 6, and 8 h using an Olympus CKX53 inverted microscope (Olympus Corporation, Japan). The scratch area was measured using ImageJ software (NIH, Bethesda, MD, USA), taking the initial value as 100% and calculating the percentage of closure.

2.7 Statistics and Analysis

The experimental results are presented as the mean $\pm$ standard deviation. Normality was assessed by the Shapiro–Wilk test. The differences between groups were tested by one-way ANOVA with Tukey's post hoc test, and the effect of the substance and concentration on cell viability and migration was tested by two-way ANOVA with the same post hoc test. $p < 0.05$ was considered significant. Data analysis was performed using GraphPad Prism 8.0 statistical analysis and visualization software (GraphPad Software, Boston, MA, USA).

3. Results and Discussion

In this study, curcumin and usnic acid were loaded into polymeric films based on hyaluronic acid (HA) of two molecular weights. A slight stimulating effect on CVCL-7036 and SK-MEL 28 melanoma cells was detected for the sample with the concentration of 10 µg/mL and HA with a higher molecular weight (Fig. 1A). However, at the concentration of 100 µg/mL, the samples with the higher molecular weight HA have the most activity against melanoma. At the low concentrations of curcumin, no therapeutic effect was observed, and probably melanoma cells break down HA into small fragments, which contributes to their activity, as some authors have found before [20,21]. The molecular weight of HA in the sample with usnic acid did not affect the activity of the sample; only dose-dependent suppression was observed.

As it is demonstrated in Fig. 1B, curcumin, even at the maximum concentration, is unable to suppress the proliferation of SK-MEL 28 cells, while the cells themselves probably contribute to the degradation of HA and thus to the enhancement of their own proliferation. However, the addition of usnic acid leads to a significant anti-proliferation effect. It is noticeable that in the samples with high molecular weight HA, the effect of usnic acid is more significant. This may be due to the fact that HA with a high molecular weight is capable of stimulating anti-inflammatory cytokine IL-10 production, suppressing tumor cell growth, and creating a physical barrier that prevents cell spread [22,23]. It is likely that in the case of the SK-MEL 28 line, only the combination of all three factors (curcumin, usnic acid, HA) contributes to the effective suppression of melanoma cells. Since the most pronounced cytotoxic effect was observed on the SK-MEL 28 melanoma cell line when incubated with HA 2.5 CUR USN at 100 µg/mL, this sample and this cell line were used in a subsequent experiment to evaluate cell migration activity in a scratch test.

Results presented in Fig. 1C demonstrate that the samples have no cytotoxic effects against HaCaT keratinocytes. On the contrary, most samples, especially those containing curcumin and usnic acid, appear to enhance cell viability. Notably, the combination of HA 1.3 with curcumin and usnic acid (HA 1.3 CUR USN) at 50 µg/mL resulted in the highest increase in metabolic activity. Since the samples of the HA 1.3 group at the concentration of 50 µg/mL maximized the viability of a healthy keratinocyte culture, these samples were chosen for further cell migration experiments.

Experiments with 1.3 and 2.5 MDa HA polymeric films and usnic acid as pure substances of our polymeric films demonstrated that the cytotoxicity of the pure components follows the same pattern as that of the composite films (Fig. 2).

HA 2.5 MDa sample in three observed concentrations has a stimulating effect on SK-MEL 28 melanoma cells. Whereas 72 h incubation with HA 1.3 MDa shows no significant effect on cell culture.

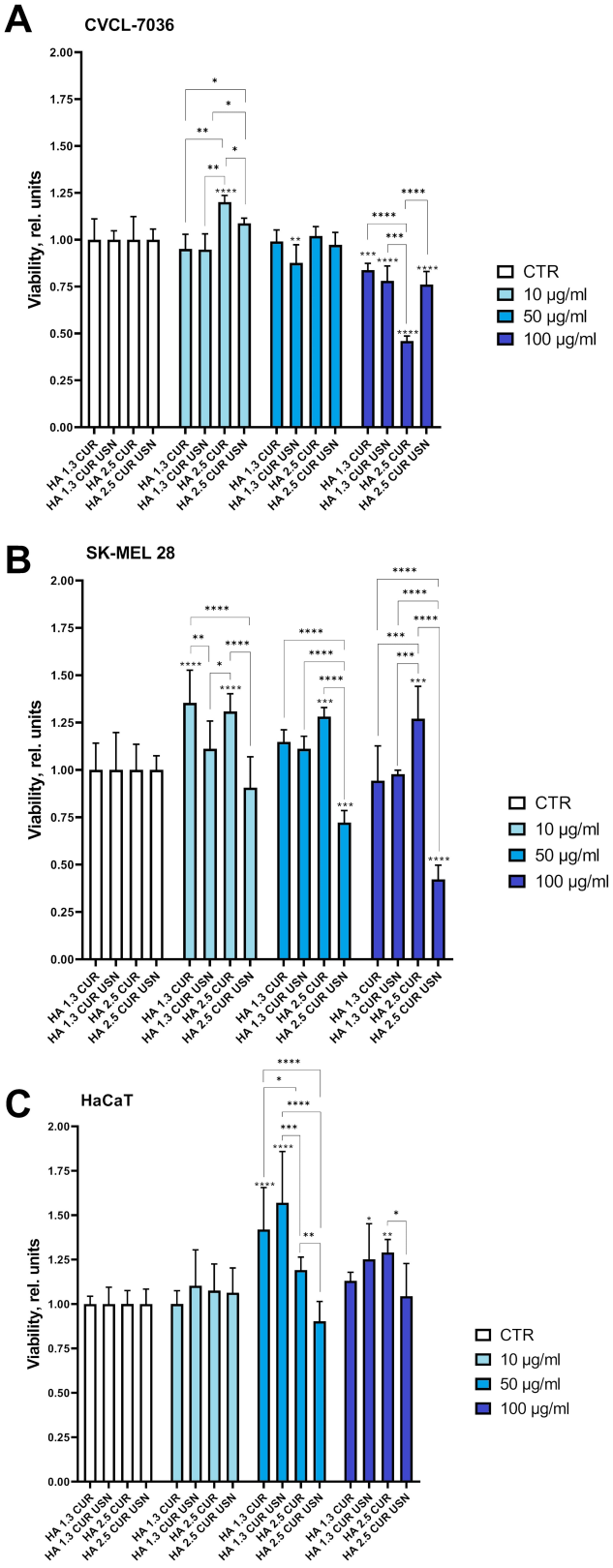

Fig. 1. Relative viability of CVCL-7036 (A), SK-MEL 28 (B), and HaCaT (C) cells after the incubation with sample solutions for 72 h at concentrations of 10, 50, and 100 µg/mL. Samples: HA 1.3 CUR, HA 1.3 CUR USN, HA 2.5 CUR and HA 2.5 CUR USN. Results represent mean ± standard deviation. Data statistical significance levels between treatment and control groups are represented by asterisks ("*" for p value < 0.05, "**" for p value < 0.01, "***" for p value < 0.001, "****" for p value < 0.0001). All samples were normalized to untreated controls.

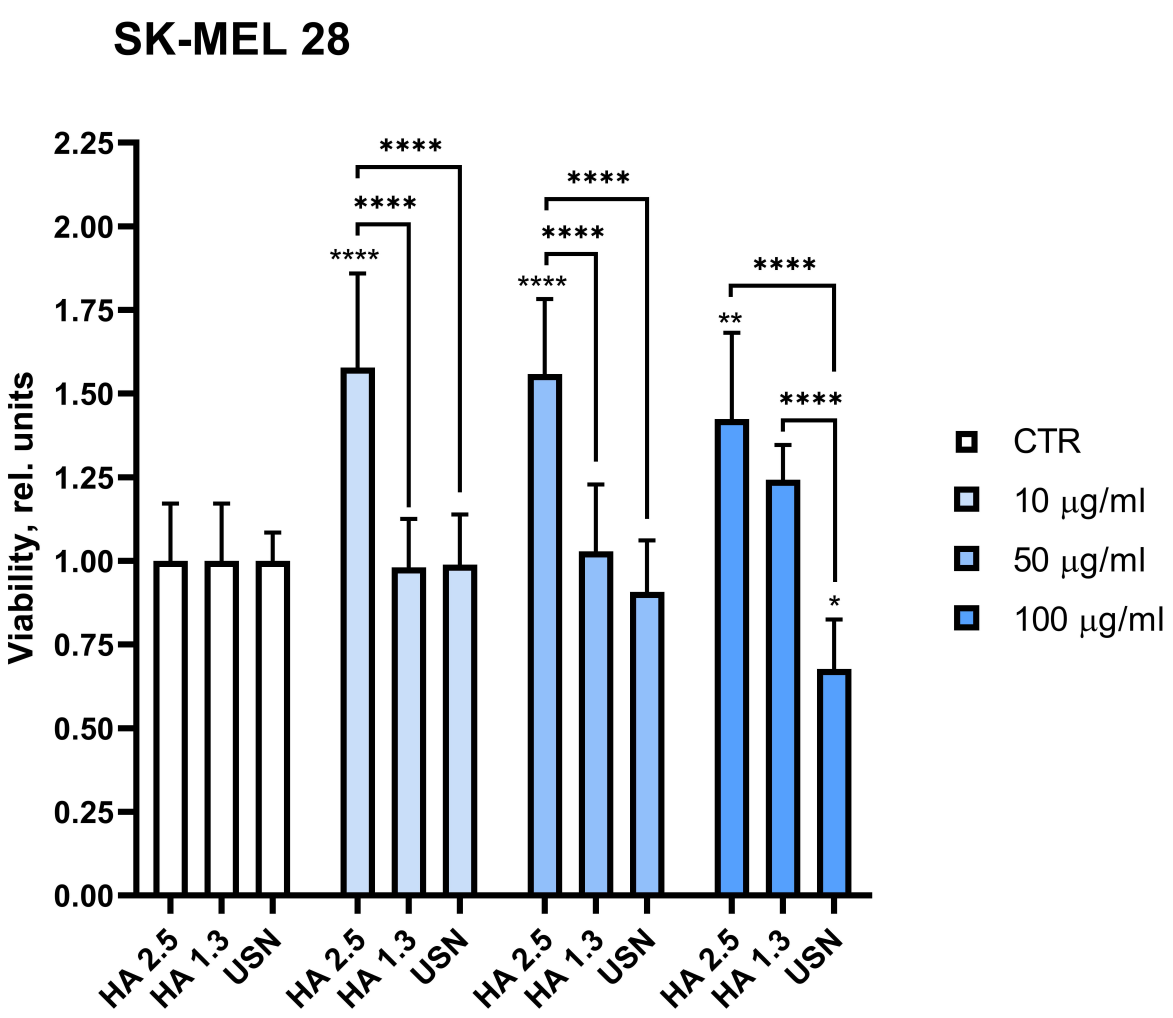

Fig. 2. Relative viability of SK-MEL 28 cells after incubation with HA 1.3, HA 2.5, and USN sample solutions for 72 h at concentrations of 10, 50, and 100 µg/mL. Results represent mean ± standard deviation. Data statistical significance levels between treatment and control groups are represented by asterisks ("*" for p value < 0.05, "**" for p value < 0.01, "****" for p value < 0.0001). All samples were normalized to untreated controls.

The cytotoxicity of pure usnic acid was studied at concentrations identical to those in polymeric film solutions 10, 50, and 100 µg/mL. Incubation with usnic acid only in the highest investigated concentration declines the SK-MEL 28 viability, whereas 50 and 100 µg/mL solutions of HA 2.5 CUR USN polymeric films reduce cells' viability. It can be explained by increasing the solubility of usnic acid associated with HA.

The analysis of cell migration demonstrates the effect of the different samples on the initial stages of scratch healing. The scratch test assessed the migratory activity of SK-MEL 28 melanoma cells based on the decrease in defect area over time. Scratch sizes were calculated from the micrographs shown in Fig. 3. The average scratch area values of the control group without added samples were compared with the groups incubated with HA 2.5 CUR USN 100 µg/mL and HA 2.5 USN 100 µg/mL (Fig. 4A,B). No significant differences from the control were detected in the scratch test data.

The analysis of cell migration demonstrates the effect of the different samples on the initial stages of scratch healing. To simulate the effect of the sample on normal keratinocytes during the wound closure with topical application, a comparison was made between the control group and two cell cultures treated with HA 1.3 CUR and HA 1.3 CUR USN sample solutions at a concentration of 50 µg/mL. The scratch area measurements were calculated from the micrographs shown in Fig. 5. The average percentages of the scratch closure are summarized in Fig. 6A,B, which illustrate the reduction of the dynamics in the scratch area over time.

In the scratch assay on HaCaT cells at the concentration of 50 µg/mL, HA 1.3 CUR and HA 1.3 CUR USN samples demonstrated a decrease in scratch area over the time comparable to the control (Fig. 5). Because the scratch assay was performed under low-serum conditions (1% FBS) and over a short time window (8 hours), the reduction in scratch area primarily reflects cell migration rather than

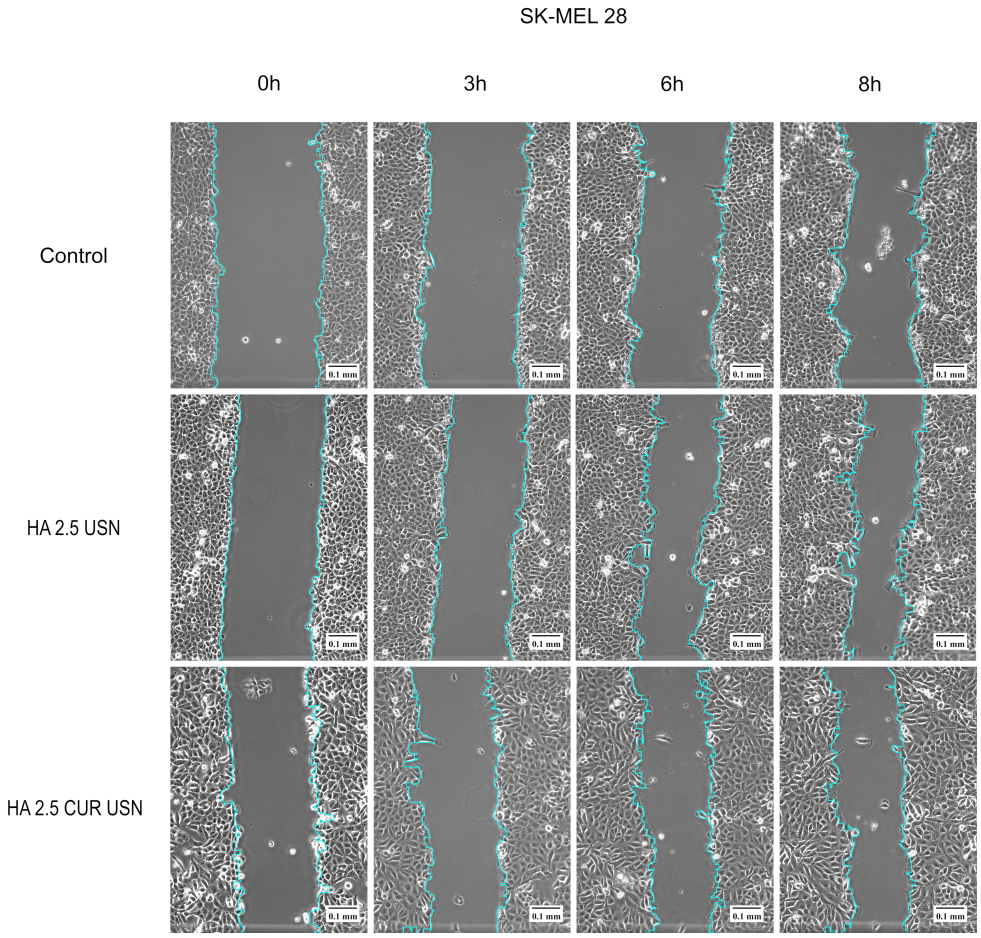

Fig. 3. Representative image of a monolayer of SK-MEL 28 melanoma cells with scratches after incubation with HA 2.5 CUR USN and HA 2.5 USN samples at a concentration of 100 µg/mL for 0, 3, 6, 8 h. Fixation of the scratch area. The edges of the scratch are outlined with a turquoise curve. Scale bar = 0.1 mm.

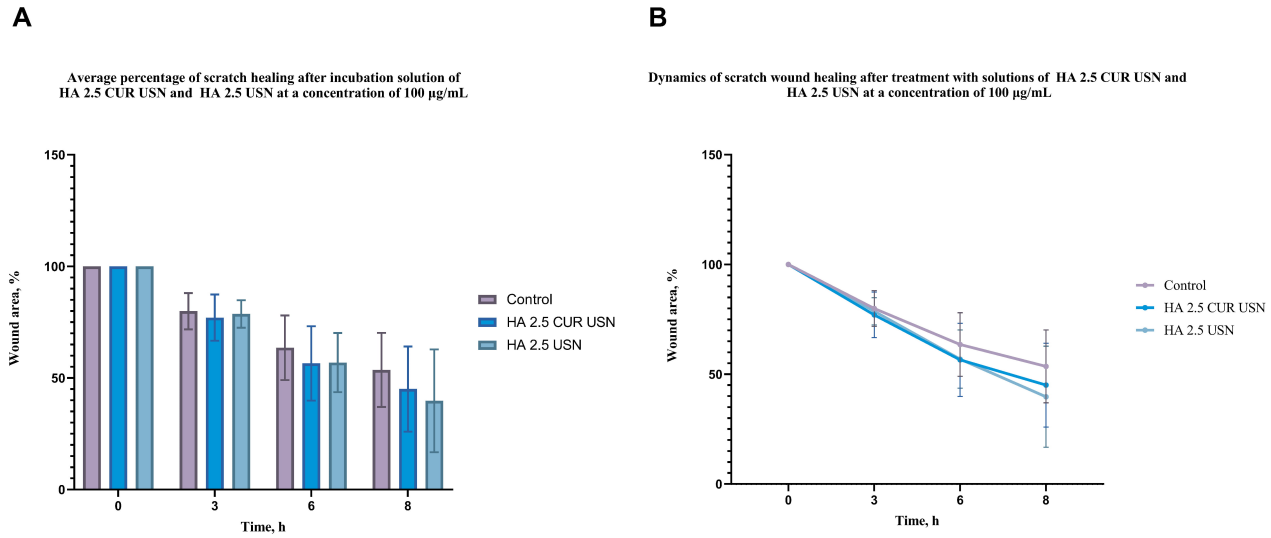

Fig. 4. The results of the comparison of the effect of HA 2.5 CUR USN and HA 2.5 USN samples with the concentration of 100 µg/mL on scratch closure in SK-MEL 28 melanoma cells, in percentage after 0, 3, 6, 8 hours. (A) Average percentage of the scratch closure in SK-MEL 28 cells. (B) Time dependence curves illustrating the dynamics of the scratch closure. Bars and dots on the graphs represent the mean ± standard deviation (n = 5). Two-way ANOVA with Tukey's post hoc test was used for the comparison.

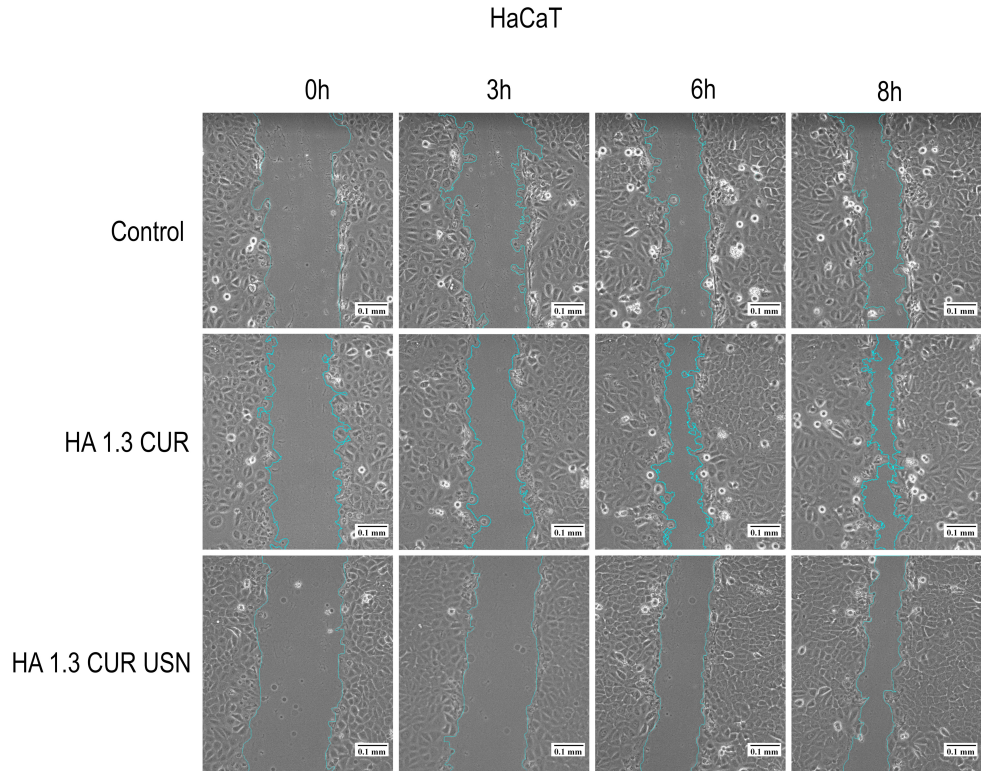

Fig. 5. Representative image of a monolayer of HaCaT cells with scratches after the incubation with the samples of the HA 1.3 group at the concentration of 50 µg/mL for 0, 3, 6, 8 h. Fixation of the scratch area—the edges of the scratch are marked with a turquoise curve. Scale bar = 0.1 mm.

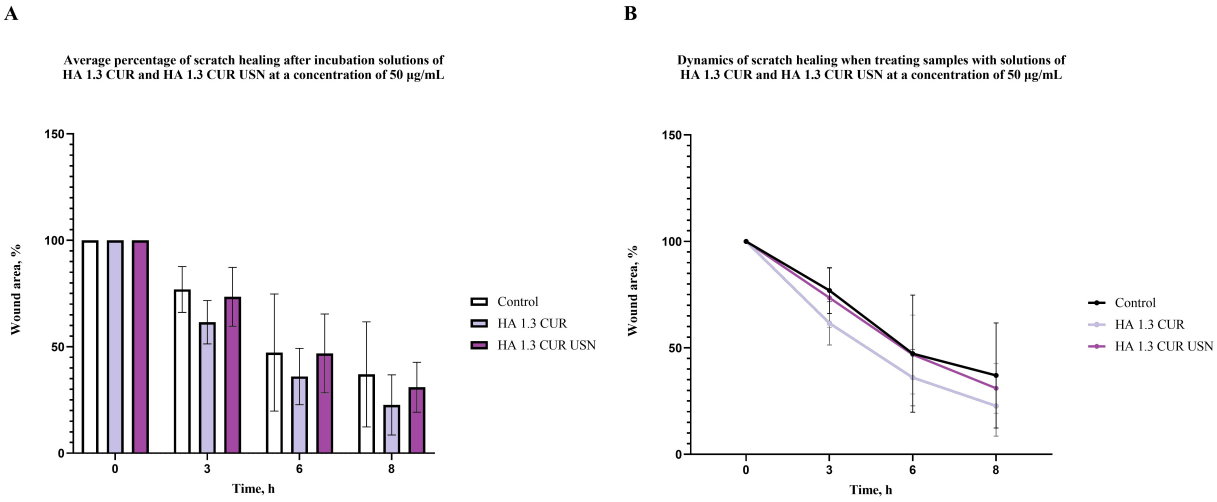

Fig. 6. The results of the comparison of the effect of HA 1.3 group samples with a solution concentration of 50 µg/mL on scratch closure on HaCaT cells after adding solutions, in percentage after 0, 3, 6, 8 hours. (A) Average percentage of scratch closure in HaCaT cells. (B) Time dependence curves illustrating the dynamics of scratch closure. Bars and dots on the graphs represent the mean ± standard deviation (n = 3). Two-way ANOVA with Tukey's post hoc test was used for comparison.

the proliferation. Despite an increase in metabolic activity (WST-1 assay) in the response to HA 1.3 CUR and HA 1.3 CUR USN, keratinocyte migration remained unchanged relative to the control. Usnic acid may influence cytoskeletal dynamics or cell adhesion properties and lead to a discrepancy between viability and motility [24].

Analysis of the biological activity of the samples with different molecular weights of hyaluronic acid (HA) showed a clear influence of the molecular weight. The samples containing HA with the molecular weight of 1.3 MDa (HA 1.3 CUR and HA 1.3 CUR USN) at the concentration of 50 µg/mL statistically significantly increased the viabil-

ity of HaCaT cells compared to the control, reaching values of 1.77 and 1.57 relative units, respectively (Fig. 1A). At the same time, the corresponding samples with HA 2.5 MDa (HA 2.5 CUR and HA 2.5 CUR USN) did not show a significant effect on the viability of HaCaT cells at all concentrations studied (Fig. 1B). A similar dependence on the HA molecular weight was also observed in the experiments on melanoma cells. Moreover, the severity of the cytotoxic effect was determined not only by the molecular weight of HA, but also by the composition of the samples, including the presence of CUR and USN. The observed differences may be associated with the peculiarities of cellular interaction and bioavailability of components in systems based on HA of the different molecular weights.

4. Conclusions

The results demonstrate that polymeric films made from natural hyaluronic acid and loaded with curcumin and usnic acid have strong potential for melanoma treatment. When curcumin and usnic acid were used together, they were synergically effective against melanoma cells such as CVCL-7036 and SK-MEL 28, while having no harmful effect on healthy skin cells (HaCaT). These films promote the growth of healthy cells. Thus, we demonstrated that the sample HA 1.3 CUR USN is effective against cancer cells and helps normal cells to survive. The study also found that the molecular weight of hyaluronic acid affects the performance of the films, influencing both on their anticancer activity and on their interaction with healthy cells. Thus, these polymeric films demonstrate both anticancer efficacy and biocompatibility, making them promising candidates for future treatments of melanoma.

Abbreviations

BRAF, human gene that encodes a protein called B-Raf; *CDKN2A*, cyclin-dependent kinase inhibitor 2A; CTLA-4, cytotoxic T-lymphocyte associated protein 4; CTR, control; CUR, curcumin; CVCL-7036, amelanotic human skin melanoma cell line; DNA, deoxyribonucleic acid; EDN1, endothelin 1; HA, hyaluronic acid; HaCaT, spontaneously immortalized keratinocyte cell line; MAPK/ERK, signaling cascade in cells that transmits signals from the cell surface to the nucleus, regulating essential cellular processes like growth, division, and differentiation; MITF, microphthalmia-associated transcription factor, a protein playing a key role in the development and function of melanocytes; p16INK4a, tumor suppressor protein, inhibitor of CDK4; P53, tumor suppressor pathway preventing the propagation of abnormal cells by regulating DNA repair, cell cycle progression, cell death, or senescence; PD-L1, 40 kDa type 1 transmembrane protein, co-inhibitory factor of the immune response; PI3K/AKT/mTOR, intracellular signaling pathway that plays a vital role in regulating cell survival, growth, proliferation, metabolism, and angiogenesis; *PTEN*, tumor suppressor gene through the action of its phosphatase protein product; ROS, reactive oxygen species; SCF, stem cell factor; SK-MEL 28, lightly pigmented human skin melanoma cell line; *TP53*, tumor suppressor gene; USN, usnic acid; UVA, ultraviolet A radiation (320–400 nm); UVB, ultraviolet B radiation (280–320 nm).

Availability of Data and Materials

The datasets used and analyzed during the current study are available from the corresponding author on reasonable request.

Author Contributions

Conceptualization: PPS, SNM, AVM, KVL; Formal analysis: ROS, HW, JZ, ZW; Investigation: PGS, KSZ, EAV, AVM, ROS; Methodology: KSZ, EAV, AVM, PPS; Visualization: ROS, KSZ, EAV, AVM; Resources: PPS, AVM, SNM; Writing — original: PGS, ROS, KSZ, KVL, AVM; Writing — review & editing: SNM, PPS; Supervision: PPS, SNM, KVL; Project administration: PPS. All authors contributed to editorial changes in the manuscript. All authors read and approved the final manuscript. All authors have participated sufficiently in the work and agreed to be accountable for all aspects of the work.

Ethics Approval and Consent to Participate

Not applicable.

Acknowledgment

We would like to thank the Laboratory of Biochemical Foundations of Pharmacology and Tumor Models from N. N. Blokhin Russian Cancer Research Center for the melanoma cell cultures.

Funding

This research was funded by the Russian Science Foundation, project number 24-23-00269. Link to information about the project: https://rscf.ru/en/project/24-23-00269/.

Conflict of Interest

The authors declare no conflict of interest.

Supplementary Material

Supplementary material associated with this article can be found, in the online version, at https://doi.org/10.31083/FBL48405.

References

[1] Timis T, Bergthorsson JT, Greiff V, Cenariu M, Cenariu D. Pathology and Molecular Biology of Melanoma. Current Issues in Molecular Biology. 2023; 45: 5575–5597. https://doi.org/10.3390/cimb45070352.

[2] Saginala K, Barsouk A, Aluru JS, Rawla P, Barsouk A. Epidemiology of Melanoma. Medical Sciences (Basel, Switzerland). 2021; 9: 63. https://doi.org/10.3390/medsci9040063.

[3] Al-Sadek T, Yusuf N. Ultraviolet Radiation Biological and Medical Implications. Current Issues in Molecular Biology. 2024; 46: 1924–1942. https://doi.org/10.3390/cimb46030126.

[4] Gieniusz E, Skrzydlewska E, Łuczaj W. Current Insights into the Role of UV Radiation-Induced Oxidative Stress in Melanoma Pathogenesis. International Journal of Molecular Sciences. 2024; 25: 11651. https://doi.org/10.3390/ijms252111651.

[5] de Oliveira NFP, de Souza BF, de Castro Coêlho M. UV Radiation and Its Relation to DNA Methylation in Epidermal Cells: A Review. Epigenomes. 2020; 4: 23. https://doi.org/10.3390/epigenomes4040023.

[6] Noonan FP, Zaidi MR, Wolnicka-Glubisz A, Anver MR, Bahn J, Wielgus A, *et al*. Melanoma induction by ultraviolet A but not ultraviolet B radiation requires melanin pigment. Nature Communications. 2012; 3: 884. https://doi.org/10.1038/ncomms1893.

[7] Liu J, Zheng R, Zhang Y, Jia S, He Y, Liu J. The Cross Talk between Cellular Senescence and Melanoma: From Molecular Pathogenesis to Target Therapies. Cancers. 2023; 15: 2640. https://doi.org/10.3390/cancers15092640.

[8] Sharma P, Goswami S, Raychaudhuri D, Siddiqui BA, Singh P, Nagarajan A, *et al*. Immune checkpoint therapy-current perspectives and future directions. Cell. 2023; 186: 1652–1669. https://doi.org/10.1016/j.cell.2023.03.006.

[9] Quek C. Genetics and Genomics of Melanoma: Current Progress and Future Directions. Genes. 2023; 14: 232. https://doi.org/10.3390/genes14010232.

[10] Motwani J, Eccles MR. Genetic and Genomic Pathways of Melanoma Development, Invasion and Metastasis. Genes. 2021; 12: 1543. https://doi.org/10.3390/genes12101543.

[11] Işlek Köklü Z, Şanverdi EL, Karadağ B, Üçişik MH, Taşkan E, Şahin F. Combinational therapy of all-trans retinoic acid (ATRA) and sphingomyelin induces apoptosis and cell cycle arrest in B16F10 melanoma cancer cells. Turkish Journal of Biology = Turk Biyoloji Dergisi. 2024; 48: 401–413. https://doi.org/10.55730/1300-0152.2715.

[12] Wawszczyk J, Jesse K, Kapral M. Pterostilbene-Mediated Inhibition of Cell Proliferation and Cell Death Induction in Amelanotic and Melanotic Melanoma. International Journal of Molecular Sciences. 2023; 24: 1115. https://doi.org/10.3390/ijms24021115.

[13] Ali ML, Roky AH, Azad SMAK, Shaikat AH, Meem JN, Hoque E, *et al*. Autophagy as a targeted therapeutic approach for skin cancer: Evaluating natural and synthetic molecular interventions. Cancer Pathogenesis and Therapy. 2024; 2: 231–245. https://doi.org/10.1016/j.cpt.2024.01.002.

[14] Wang M, Jiang S, Zhou L, Yu F, Ding H, Li P, *et al*. Potential Mechanisms of Action of Curcumin for Cancer Prevention: Focus on Cellular Signaling Pathways and miRNAs. International Journal of Biological Sciences. 2019; 15: 1200–1214. https://doi.org/10.7150/ijbs.33710.

[15] Zhao G, Han X, Zheng S, Li Z, Sha Y, Ni J, *et al*. Curcumin induces autophagy, inhibits proliferation and invasion by downregulating AKT/mTOR signaling pathway in human melanoma cells. Oncology Reports. 2016; 35: 1065–1074. https://doi.org/10.3892/or.2015.4413.

[16] Rancan F, Rosan S, Boehm K, Fernández E, Hidalgo ME, Quihot W, *et al*. Protection against UVB irradiation by natural filters extracted from lichens. Journal of Photochemistry and Photobiology. B, Biology. 2002; 68: 133–139. https://doi.org/10.1016/s1011-1344(02)00362-7.

[17] Wang H, Xuan M, Huang C, Wang C. Advances in Research on Bioactivity, Toxicity, Metabolism, and Pharmacokinetics of Usnic Acid In Vitro and In Vivo. Molecules (Basel, Switzerland). 2022; 27: 7469. https://doi.org/10.3390/molecules27217469.

[18] Galanty A, Zagrodzki P, Gdula-Argasińska J, Grabowska K, Koczurkiewicz-Adamczyk P, Wróbel-Biedrawa D, *et al*. A Comparative Survey of Anti-Melanoma and Anti-Inflammatory Potential of Usnic Acid Enantiomers-A Comprehensive In Vitro Approach. Pharmaceuticals (Basel, Switzerland). 2021; 14: 945. https://doi.org/10.3390/ph14090945.

[19] Grada A, Otero-Vinas M, Prieto-Castrillo F, Obagi Z, Falanga V. Research Techniques Made Simple: Analysis of Collective Cell Migration Using the Wound Healing Assay. The Journal of Investigative Dermatology. 2017; 137: e11–e16. https://doi.org/10.1016/j.jid.2016.11.020.

[20] Voelcker V, Gebhardt C, Averbeck M, Saalbach A, Wolf V, Weih F, *et al*. Hyaluronan fragments induce cytokine and metalloprotease upregulation in human melanoma cells in part by signalling via TLR4. Experimental Dermatology. 2008; 17: 100–107. https://doi.org/10.1111/j.1600-0625.2007.00638.x.

[21] Sapudom J, Nguyen KT, Martin S, Wippold T, Möller S, Schnabelrauch M, *et al*. Biomimetic tissue models reveal the role of hyaluronan in melanoma proliferation and invasion. Biomaterials Science. 2020; 8: 1405–1417. https://doi.org/10.1039/c9bm01636h.

[22] Shi Q, Zhao L, Xu C, Zhang L, Zhao H. High Molecular Weight Hyaluronan Suppresses Macrophage M1 Polarization and Enhances IL-10 Production in $PM_{2.5}$-Induced Lung Inflammation. Molecules (Basel, Switzerland). 2019; 24: 1766. https://doi.org/10.3390/molecules24091766.

[23] Michalczyk M, Humeniuk E, Adamczuk G, Korga-Plewko A. Hyaluronic Acid as a Modern Approach in Anticancer Therapy-Review. International Journal of Molecular Sciences. 2022; 24: 103. https://doi.org/10.3390/ijms24010103.

[24] Burlando B, Ranzato E, Volante A, Appendino G, Pollastro F, Verotta L. Antiproliferative effects on tumour cells and promotion of keratinocyte wound healing by different lichen compounds. Planta Medica. 2009; 75: 607–613. https://doi.org/10.1055/s-0029-1185329.